



Impurity-related vibrational modes in a pentacene crystal

G. Volonakis, L. Tsetseris, S. Logothetidis

► To cite this version:

G. Volonakis, L. Tsetseris, S. Logothetidis. Impurity-related vibrational modes in a pentacene crystal. European Physical Journal: Applied Physics, 2011, 55 (2), <10.1051/epjap/2011100423>. <hal-00723600>

HAL Id: hal-00723600

<https://hal.science/hal-00723600v1>

Submitted on 11 Aug 2012

HAL is a multi-disciplinary open access archive for the deposit and dissemination of scientific research documents, whether they are published or not. The documents may come from teaching and research institutions in France or abroad, or from public or private research centers.

L'archive ouverte pluridisciplinaire **HAL**, est destinée au dépôt et à la diffusion de documents scientifiques de niveau recherche, publiés ou non, émanant des établissements d'enseignement et de recherche français ou étrangers, des laboratoires publics ou privés.



HAL Authorization

Impurity-related vibrational modes in a pentacene crystal

G. Volonakis^{1,a}, L. Tsetseris^{2,3}, and S. Logothetidis¹

¹Department of Physics, Aristotle University of Thessaloniki, Thessaloniki, Greece

²Department of Physics, National Technical University of Athens, Athens, Greece

³Department of Physics and Astronomy, Vanderbilt University, Nashville, TN, USA

^a *Corresponding author*, phone number: +30-2310-998239, email:gvolo@physics.auth.gr

Abstract

The presence of impurities in the molecular crystals of organic semiconductors is a key limiting factor for the performance of related electronic devices. For this reason, the atomic-scale details of impurity incorporation are important elements for modeling and optimization of organic electronic systems. In this article, we use first-principles density-functional theory calculations to describe the vibrational spectrum of typical impurity culprits in the prototype organic semiconductor pentacene. First, we validate the computational approach by comparing results on vibrational modes of impurity-free pentacene with available theoretical and experimental data. We then analyze the effect of oxygen, water, and hydrogen impurities on the modes of pentacene crystals. The results identify distinct impurity-related features which can help understand the evolution of impurities in pentacene samples.

1. Introduction

The degradation of organic electronic systems due to the presence of defects and chemical impurities has long been recognized as one of the most important hindering factors for the development of associated electronic devices [1-3]. For example, experimental data on oxygen insertion and reactions in various organic semiconductors show that these processes create traps for charge carriers, limiting mobility and degrading transport characteristics [4-9]. Theoretical studies have probed the effect of impurities on the electronic properties of organic materials, and, in certain cases, found agreement with available experimental data. Examples include the creation of carrier traps due to oxygen incorporation in pentacene, rubrene, or C₆₀ fullerite crystals [10-14]. However the existence of a large number of possible impurity configurations creates the need to

test the atomic-scale structural details of these configurations against pertinent experimental data. Specifically, comparison between theoretical and experimental Raman or infrared spectroscopic data can enable the identification of impurity structures and ultimately lead to methods that restrict impurity-related degradation phenomena.

In this article, we use quantum-mechanical first-principles calculations to obtain the vibrational modes of oxygen, water, and hydrogen-related impurities in pentacene, a widely used small-molecule organic semiconductor. Previous theoretical and experimental studies [15-18] have probed the vibrational modes of pristine pentacene, but results on related impurity effects remain missing. These results are described below for a number of modes that differ in the chemical form and the position of impurities in a pentacene crystal.

2. Methodology

The calculations employed the density-functional theory (DFT) code VASP [19]. Ultrasoft pseudopotentials were used to describe the interactions between the valence electrons and ionic cores, [20] while the exchange and correlation interactions of the valence electrons were described through a local-density approximation (LDA) [21] functional. The energy cutoff was set at 400 eV. For the calculations of the vibrational modes for pristine pentacene crystal, we used a unit cell containing 2 molecules as proposed by Campbell et al. [22,23] and a $2 \times 2 \times 2$ k-point grid. Impurity calculations employed $2 \times 2 \times 1$ supercells in terms of the unit cell, containing 8 pentacene molecules per supercell and the Γ point for k-point sampling. Vibrational modes that were calculated with a finer $2 \times 2 \times 2$ k-grid differ from those obtained with Γ point sampling by less than 3 cm^{-1} . Vibrational modes were obtained as eigenvalues of the dynamical matrix, and included two-point finite differences with displacements away from the equilibrium positions of atoms. Convergence was confirmed both for more displacements and different step sizes.

3. Results and discussion

3.1 Impurity-free pentacene

Based on the experimental data on the so-called solution phase [22,23], the lattice parameters for crystalline unit cell were set at $a=6.06 \text{ \AA}$, $b=7.9 \text{ \AA}$, $c=14.88 \text{ \AA}$, $\alpha=96.77^\circ$, $\beta=100.54^\circ$ and $\gamma=94.2^\circ$. Optimization of the structure of pentacene molecules within a unit-cell of the crystal yielded C-C bond lengths in the range of 1.36 \AA to 1.44 \AA . These bond lengths are in excellent agreement with previous *ab initio* ($1.37\text{--}1.46 \text{ \AA}$) and experimental studies ($1.35\text{--}1.45 \text{ \AA}$) [16,22].

Before analyzing impurity-related effects, let us discuss results on selected vibrational modes of an isolated impurity-free pentacene molecule. The two modes shown in Figs. 1a-b

have frequencies of 1170 cm^{-1} and 1136 cm^{-1} , respectively, and they correspond to vibrations of H-atoms within the molecular plane. The corresponding frequency values in previous theoretical (experimental) studies were 1223 (1178) and 1194 (1158) cm^{-1} [15]. The Raman-active mode depicted in Fig. 1c, on the other hand, has a frequency of 265 cm^{-1} , while previous calculated and measured values placed this eigenvalue at 263 and 266 cm^{-1} [16], respectively.

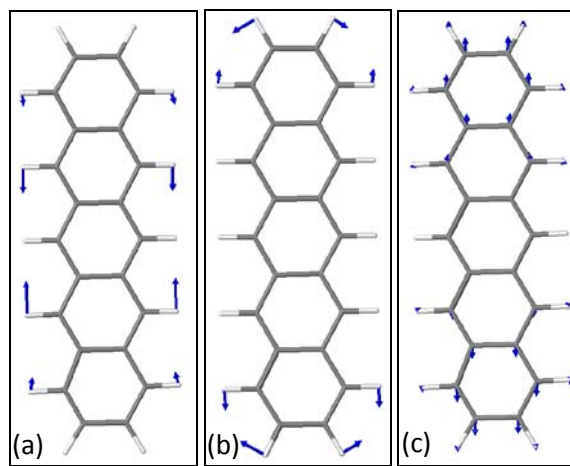


Figure 1. Selected vibrational modes for an isolated pentacene molecule with frequencies 1170 (a), 1136 (b) and 265 cm^{-1} (c)

The close agreement between our results and those of previous studies reinforce the validity of the computational approach employed here for the analysis of impurity effects.

3.2 Oxygen Impurities

Total-energy DFT calculations [10] on O_2 insertion in pentacene crystals identified two dissociated forms of pairs of O atoms as the most stable configurations. These configurations include the pair of epoxy bridges shown in Fig. 2(a) (O_I) and inter-molecular bridge structure of Fig. 2(b) (O_{II}). Moreover, since the dissociation energy [10] of oxygen pairs to individual O impurities is very small ($\sim 0.1 \text{ eV}$), the atomic O structures depicted in Fig. 1c (O_{III}) and Fig. 1d (O_{IV}) are as energetically favorable as the geometries O_I and O_{II} . Oxygen impurities in these

configurations cause displacements of neighboring atoms off their equilibrium positions. In particular removal of the O impurities causes relaxation of up to 0.48, 0.57, 0.74 and 0.72 Å for vicinal atoms in structures O_I, O_{II}, O_{III} and O_{IV}, respectively. For other atoms of the same molecule maximum displacements are 0.35, 0.3, 0.44 and 0.45 Å, whereas the corresponding values for atoms of neighboring molecules are 0.23, 0.29, 0.32 and 0.31 Å.

In order to calculate the vibrational modes of these impurity configurations we constructed the dynamical matrix including the degrees of freedom associated with the O atoms and their nearest C atoms. It should be noted that Figures depict only the molecule or molecules that accommodate the impurities, even though the calculations of the vibrational modes take into account the complete crystalline environment with all the surrounding pentacene molecules.

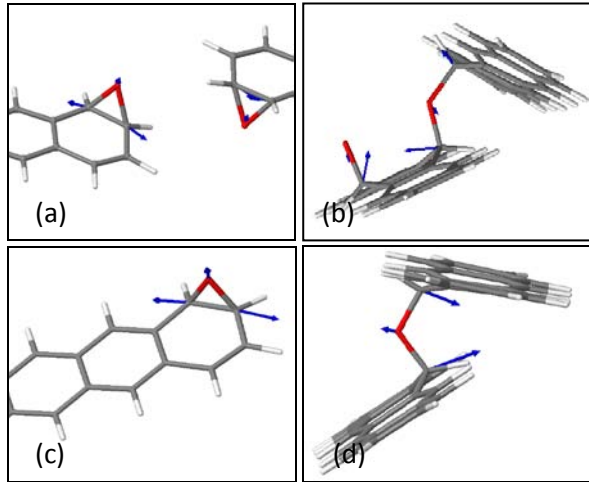


Figure 2. Selected vibrational modes of the O-pair structures O_I (a) and O_{II} (b) and atomic O configurations O_{III} (c) and O_{IV} (d).

Vibrational modes of defects for structures O_{II}, O_{III}, and O_{IV} are given in Table 1. The type of vibrations for the highest energy modes of all structures are depicted in Figs. 2a-d. These modes have frequencies of 1385, 1229, 1389, and 1181 cm⁻¹, respectively. As expected, the frequencies calculated for the modes of

structures O_I (not shown) and O_{III} are almost identical (within 10 cm⁻¹), but this is not the case for O_{II} and O_{IV}. Likewise, the two atomic oxygen configurations, O_{III} and O_{IV} differ significantly in terms of frequencies. Those features suggest that experimental studies can distinguish not only the form of oxygen-related impurity configurations, but also whether it is energetically favorable for oxygen in pentacene to appear in pairs or as individual impurities

TABLE 1: Vibrational modes for O₂ into pentacene crystal, structures O_{II}, O_{III}, and O_{IV}

mode	O _{II} Freq. (cm ⁻¹)	O _{III} Freq. (cm ⁻¹)	O _{IV} Freq. (cm ⁻¹)
1	1229	1389	1181
2	1147	1198	1121
3	1110	1072	1061
4	1056	899	1026
5	1043	860	951
6	1014	656	855
7	1005	438	587
8	915	429	562
9	884	370	377

3.3 H₂O-related impurities

In the case of H₂O-related impurities, we considered two structures [10] wherein the water molecule stays intact (physisorbed). One between pentacene layers, which is the stablest (W_I) and another where H₂O is between adjacent pentacene molecules in the same layer (W_{II}). For the latter case the formation energy rises by 0.5 eV.

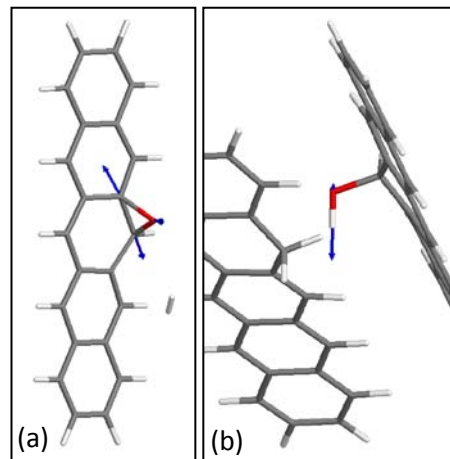


Figure 3. Vibrational modes of chemisorbed H₂O impurities: (a) forming COC bond and H₂, (b) forming COH bond and CH₂ group.

The frequencies of the vibration modes are given in Table 2. We are noticing a reduction of the frequencies for the stretching modes when H₂O molecule is between molecules and a slight increase of the frequency for the bending mode. These small differences can thus clarify whether water molecules reside inside pentacene layers or between the layers in a particular experiment. Both these possibilities have been reported in previous studies [9,24].

TABLE 2: Normal modes for a physisorbed H₂O molecule in a pentacene crystal.

Mode	H ₂ O between layers Freq. (cm ⁻¹)	H ₂ O between molecules Freq. (cm ⁻¹)
asymmetric stretch	3747	3659
symmetric stretch	3564	3548
Bending	1466	1474

Next the case of two chemisorbed configurations for H₂O impurities was studied. First, a water molecule dissociates into a COC group and H₂ (Fig. 3a, W_{III}) while for the second the dissociation leads to a COH and a CH₂ group (Fig. 3b, W_{IV}). Compared to the most stable configuration W_I, these chemisorbed structures have energies that are higher by 1.2 and 3.1 eV, respectively. They are thus metastable that can exist only under non-equilibrium conditions, perhaps during synthesis. The results for the vibrational modes for the COC group of structure W_{III} and the CH₂ group of W_{IV} are presented in Table 3.

TABLE 3: Vibrational modes for chemisorbed H₂O impurities in pentacene crystal structures

mode	COC in W _{III} Freq. (cm ⁻¹)	CH ₂ in W _{IV} Freq. (cm ⁻¹)	CH ₂ Freq. (cm ⁻¹)
1	1319	2969	2936
2	1173	2864	2865
3	1046	1317	1322
4	908	1267	1264
5	764	1126	1121

6	643	881	871
7	441	836	790
8	434	730	737
9	363		

As can be deduced from a comparison between the results of Tables 2 and 3, the frequencies of the W_{III} modes are smaller from the corresponding values of the eigenvalues for the COC group of the O_I configuration. This decrease is associated with the fact that the COC group occupies different sites in the two cases. In particular, the epoxy structure is located at the center ring in the W_{III} case, while for O_I it is found at the edge of the molecule.

Finally, we discuss the vibrational modes of an H atom that is absorbed in the form of CH₂ unit, as shown in Fig. 4. Such H-related defects are known to add levels in the gap [10,11,24] and thus are crucial for transport properties of pentacene.

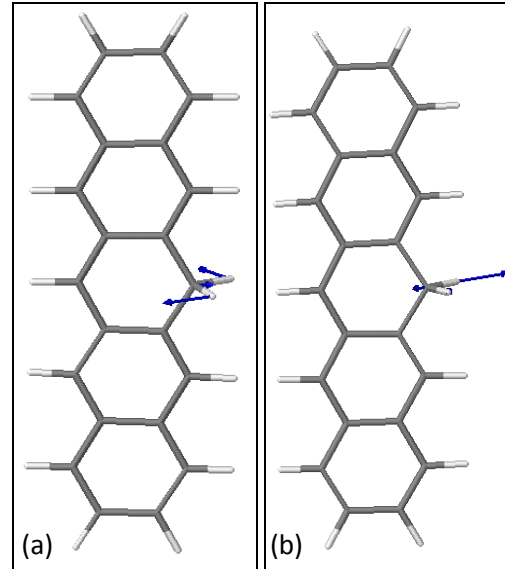


Figure 4. Bending mode of CH₂ in pentacene crystal (a) and CH stretching mode of the CH₂ group (b).

The eigenvalues of this impurity structure are included in Table 3 and they are, naturally, similar to the frequencies obtained for the CH₂ group of the structure W_{IV}. For example, the CH₂ bending mode for the H ad-atom structure, shown in Fig. 4a, has a frequency of 1322 cm⁻¹ while for W_{IV} the same mode has 1317 cm⁻¹. Frequencies of the CH stretching

modes for both this structure (Fig. 4b) and W_{IV} , are calculated 2936, 2969 and 2865, 2864 cm^{-1} (Table 3). Those are found to be lower than in pristine pentacene ($>3040 \text{ cm}^{-1}$).

As noted above, comparison between theoretical values for vibrational frequencies and pertinent experimental data can help identify the atomic scale details of impurity configurations. For example, several O-related modes (1072, 884, 860, 855, 656, 370, 377 cm^{-1}) lie outside the intrinsic vibrational bands of pentacene [16] and may thus be detected in IR or Raman spectroscopy experiments. Likewise, there are H_2O -related modes (1267, 881, 363 cm^{-1}) which do not overlap with the modes of the host pentacene crystal.

4. Summary

In summary, we have calculated the vibrational modes of pristine pentacene and pentacene crystals with hydrogen, oxygen and water-related impurities. Variations in the position and structural form of the impurities give rise to differences in vibrational frequencies and can enable the characterization of these defects in pentacene.

The calculations used resources of the EGEE and HellasGrid infrastructure.

5. References

- [1] D. Knipp, J. Appl. Phys. **101** 044504 (2007).
- [2] Z. Zhu, Applied Phys. Lett. **81** 4643 (2002).
- [3] M. Rusu, Appl. Phys. Lett. **90** 153511 (2007).
- [4] O. Mitrofanov, Phys. Rev. Lett. **97** 166601 (2006).
- [5] Y.S. Yang, Appl. Phys. Lett. **80** 1595 (2002).
- [6] A. Maliakal, Chem. Mat. **16** 4980 (2004).
- [7] C. Lee, Phys. Rev. B **49** 10572 (1994).
- [8] T. Matsushima, Appl. Phys. Lett. **91** 103505 (2007).
- [9] O.D. Jurchescu, , Applied Physics Letters **87** 052102 (2005).
- [10] L. Tsetseris, Phys. Rev. B **75** 153202 (2007).
- [11] J. Northrup, Phys. Rev. B **68** 041202 (2003).
- [12] L. Tsetseris, Phys. Rev. B **78** 115205 (2008).
- [13] L. Tsetseris, Org. Electron. **10** 333 (2009).
- [14] L. Tsetseris, Phys. Rev. B **82** 045201 (2010).
- [15] H. Cheng, Org. Electron. **10** 289 (2009).
- [16] Y. Yamakita, J. Chem. Phys. **126** 064904 (2007).
- [17] S.R. Langhoff, J. Phys. Chem. **100** 2819 (1996).
- [18] R. He, Appl. Phys. Lett. **94** 223310 (2009).
- [19] G. Kresse, Phys. Rev. B, Condensed Matter **54** 11169 (1996).
- [20] D. Vanderbilt, Phys. Rev. B **41** 7892 (1990).
- [21] J. Perdew, Phys. Rev. B **23** 5048 (1981).
- [22] R. Campbell, Acta Cryst. **14** 705 (1961).
- [23] R. Campbell, Acta Cryst. **15** 289 (1962).
- [24] K. Lee, Surf. Sci. **603** 3445 (2009).
- [25] D. Lang, Phys. Rev. Lett. **93** 076601 (2004).